Research Article | Vol. 27, No. 14 | 8 Jul 2019 | OPTICS EXPRESS 19486
Optics EXPRESS

Multi-point dynamic strain sensing using external modulation-based Brillouin optical correlation domain analysis

BHARGAV SOMEPALLI,[1,2] DEEPA VENKITESH,[1] CHAO LU,[2] AND BALAJI SRINIVASAN[1,*]

[1] *Department of Electrical Engineering, Indian Institute of Technology Madras, Chennai 600036, India*
[2] *Photonics Research Centre, Department of Electronic and Information Engineering, The Hong Kong Polytechnic University, Hong Kong, China*
[*] *balajis@ee.iitm.ac.in*

Abstract: We report a novel technique to detect dynamic strain variations simultaneously at multiple locations. Our technique is based on Brillouin optical correlation domain analysis implemented through external modulation to generate multiple independently-accessible correlation peaks within the sensing fiber. Experiments are carried out to demonstrate the precise determination of Brillouin frequency shift (BFS) from multiple locations independently. As a proof of principle, two correlation peaks are generated within a 1 km long fiber and their independent tunability is verified experimentally by mapping the spatial profile of the two correlations. We also experimentally demonstrate the detection of dynamic strain variations at two locations simultaneously, each with a spatial resolution of 60 cm over 100 m long fiber.

1. Introduction

Stimulated Brillouin scattering (SBS) based sensors have been extensively studied and implemented in the past few decades for distributed measurement of strain and/or temperature [1–5]. Specifically, Brillouin optical correlation domain analysis (BOCDA) [6, 7] has been widely used for dynamic strain sensing applications requiring sub-meter spatial resolution [8] such as load monitoring of aircrafts [9]. In BOCDA, a frequency-modulated [10] or phase-modulated [11] narrow linewidth laser source is split into two to generate the pump and probe lightwaves. These two lightwaves are counter propagated in the fiber under test (FUT) thereby localizing the SBS process through correlation peaks formed at specific periodic locations.

Conventional frequency-modulated BOCDA sensors employ direct modulation of a narrow linewidth laser source such as a distributed feedback (DFB) laser to generate frequency modulated (FM) pump and probe [12]. This technique is useful to generate only one independent correlation peak within the FUT, thus limiting the measurements to a single location at any given instance. Distributed sensing is achieved by sweeping the same correlation peak along the FUT by varying the modulation frequency (f_m) [13]. However, several structural health monitoring applications require faster measurements (~100 Hz) as well as more number of sensing points. This can be addressed by enabling simultaneous measurements at multiple independent locations. Several configurations have been demonstrated to monitor multiple locations. In random access BOCDA technique [14], modulation frequency is switched between different values and the corresponding sensing locations are accessed alternately, but sequentially. In temporal gating BOCDA technique [15, 16], the FM modulation is done with larger modulation frequency such that multiple correlation peaks are generated within the FUT. However, changing the modulation frequency changes the location of all the correlation peaks making the location of each correlation peak dependent on that of the other. The information from each of these correlation peaks are separated by temporally gating the pump lightwave. Hence, multiple locations are monitored

#366481 https://doi.org/10.1364/OE.27.019486
Journal © 2019 Received 1 May 2019; revised 11 Jun 2019; accepted 12 Jun 2019; published 26 Jun 2019

Optics EXPRESS

sequentially in all the above configurations, thereby limiting the measurement speed. We recently proposed external phase modulation-based BOCDA technique where multiple correlation peaks are generated within the FUT whose individual locations can be tuned independent of the other thereby enabling monitoring of multiple independent locations simultaneously [17]. We also experimentally demonstrated the generation and independent control of multiple correlation peaks within the FUT [17].

In this paper, we demonstrate the use of external modulation-based BOCDA to measure dynamic strain events at different locations in the sensing fiber. To the best of our knowledge, this is the first ever experimental demonstration of independent control of multiple correlation peaks in BOCDA which enables simultaneous multi-point dynamic strain sensing. We present the experimental results on extracting the Brillouin gain spectrum (BGS) from multiple correlation peak locations independently. Static and dynamic strain variations are applied to the FUT and the corresponding changes in the Brillouin frequency shift (BFS) are detected simultaneously at two different spatial locations using external modulation-based BOCDA. The paper is organized as follows. The principle of external modulation-based BOCDA is discussed in Section 2. The experimental details and the corresponding results to demonstrate the extraction of strain variations from multiple correlation peak locations are discussed in subsequent sections. This is followed by conclusions from this work.

2. Principle of external modulation-based BOCDA

The BOCDA system typically uses direct modulation of a narrow linewidth source with sinusoidal signal to achieve frequency modulated pump and probe, which in turn results in periodic correlation events along the length of the sensing fiber. The separation between the adjacent correlation peaks (d) is given by [18]

$$d = \frac{c}{2nf_m} \sim \frac{10^8}{f_m}, \tag{1}$$

where c is the speed of light in vacuum, n is the effective index of the fundamental mode in fiber and f_m represents the modulation frequency. The location of the correlation peaks (except for the zeroth order peak located at the center of the fiber) can be tuned by changing the modulation frequency f_m. The spatial resolution (Δz) of the BOCDA system, which corresponds to the spatial range over which the spectral width of the pump-probe beat spectrum is twice the Brillouin linewidth is given by [18]

$$\Delta z = \frac{c\Delta\nu_B}{2\pi n f_m \Delta f}, \tag{2}$$

where $\Delta\nu_B$ is the Brillouin gain bandwidth ($\sim$ 30 MHz) and Δf is the frequency deviation. Thus, for a given fiber, the location of sensing is solely determined by the modulation frequency, while the spatial resolution is additionally influenced by the frequency deviation. In order to have unambiguous and reliable sensing in a given length of FUT, the modulation frequency is chosen such that only one correlation order is supported within the FUT. One of the two lightwaves - pump or probe, is delayed relative to the other such that the correlation event generated within the FUT corresponds to non-zeroth interaction and hence can be tuned across the FUT for distributed sensing. In order to monitor multiple locations simultaneously, multiple correlation peaks corresponding to the same correlation order have to be generated within the FUT. This would require optical modulation with signals that have different f_m values, each of which would uniquely determine a sensing location. Additionally, each of these correlation peaks have to be tuned independently in order to monitor the user-specified locations. Direct modulation of laser is not amicable to the above constraints, the mathematical details of how an external modulator can be used for generating multiple correlation peaks simultaneously, are discussed in the Appendix A.

Optics EXPRESS

In this work, we generate the requisite sinusoidal FM signals with unique sets of f_m and Δf in the electrical domain using an arbitrary waveform generator and embed these features in the optical domain through an external phase modulator (PM). Although the principle explained in this section and the demonstrations in subsequent sections are based on using phase modulator, the same can be implemented using an intensity modulator.

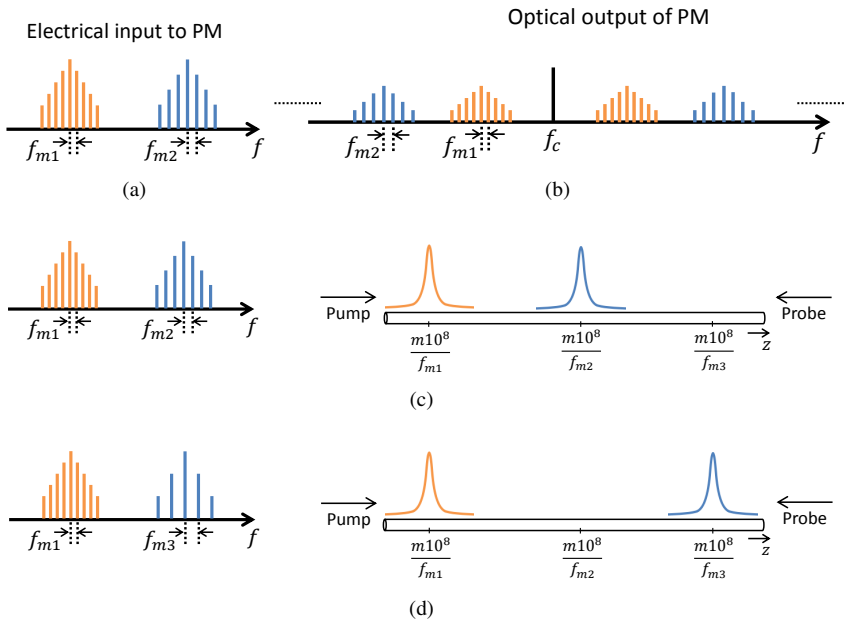

Fig. 1. Mechanism of generating multiple FM signals using external phase modulation. (a) Typical frequency spectra of an electrical signal with FM modulation at different center frequencies and (b) corresponding output spectrum of optical phase modulator. (c-d) Independent tunability of correlation peaks by modifying the modulation frequency of one of the FM signals from f_{m2} to f_{m3}.

An optical phase modulator when driven by an electrical signal generates multiple sidebands with a spectral content similar to that of the driving electrical signal. The electrical drive signal that can generate multiple correlation peaks is comprised of multiple FM signals at distinct center frequencies and with different values of f_m. The typical structure of the frequency spectrum of the drive signal when it consists of two modulation frequencies corresponding to f_{m1} and f_{m2} is shown in Fig. 1(a) and the corresponding output of the phase modulator is shown in Fig. 1(b). The frequency deviation Δf decides the strength of the side bands for each FM set. If the FM sets are within the bandwidth of the phase modulator, the optical output of the same is expected to have optical carrier (at f_c) and multiple FM signals on both sides of the optical carrier with same f_m frequencies as in the electrical domain. When such an optical signal is used to generate the pump and the probe in a Brillouin sensing experiment, each of these multiple FM signals generates a corresponding correlation peak whose location and width are determined by the respective f_m and Δf values. The location of each correlation peak can be tuned independent of the other by modifying the corresponding FM signal in the electrical domain as shown in Figs. 1(c) and 1(d).

Driving the external modulator with two FM signals with modulation frequencies f_{m1} and f_{m2} (as shown in Fig. 1(c)) generates two correlation peaks at locations given by Eq. (1). When the modulation frequency of one of the FM signals is modified from f_{m2} to f_{m3}, the location

Optics EXPRESS

of the corresponding correlation peak alone can be changed as shown in Fig. 1(d). Thus by driving the external modulator using multiple FM signals and with a careful choice of f_m values, multiple independently-addressable correlation peaks can be generated at specific locations across the sensing fiber, thereby enabling the ability to monitor multiple locations simultaneously. Even though the illustrations shown in Fig. 1 indicate distinct center frequencies for different FM signals, the difference between the center frequencies do not influence the measurement result; they could in fact be identical in an experiment. Since the signal from each correlation peak is characterized by a modulation frequency f_m, independent acquisition of information corresponding to each peak is possible using lock-in detection. It should be noted that since both the pump and the probe are modulated with the same frequency f_m and are counter-propagating, the strongest signature for lock-in detection would correspond to a frequency of $2f_m$. This is validated through simulations discussed in Appendix B.

3. Experimental details

A schematic diagram of the experimental setup used to monitor multiple locations using external modulation-based BOCDA is shown in Fig. 2. A narrowband laser (Coherent Solutions -

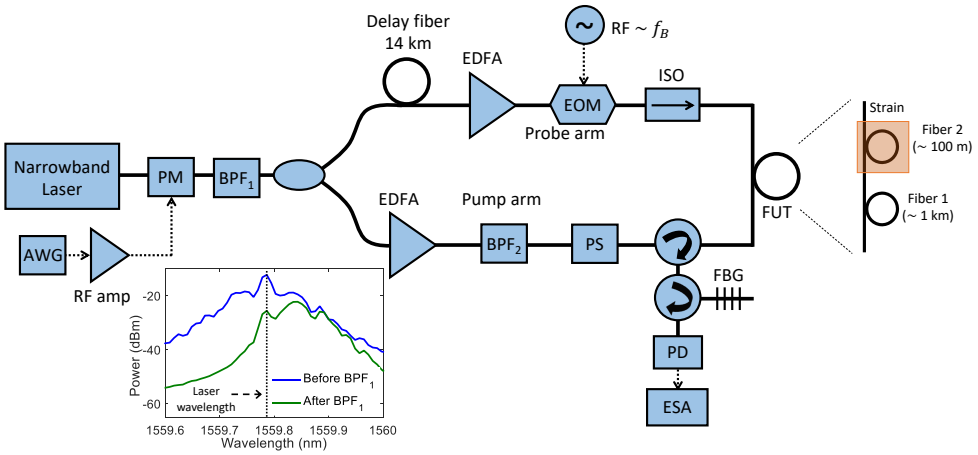

Fig. 2. Schematic of the experimental setup and the fiber under test. The optical spectra before and after the BPF_1 are shown in the inset; PM: Phase modulator; AWG: Arbitrary waveform generator; BPF: Bandpass filter; EDFA: Erbium-doped fiber amplifier; EOM: Electro-optic modulator; ISO: Optical isolator; PS: Polarization scrambler; FBG: Fiber Bragg grating; PD: Photo detector; ESA: Electrical spectrum analyzer.

linewidth 25 kHz) at a wavelength of ~1560 nm is used as the light source. The output of the laser is modulated using an external phase modulator (Photline - MPZ-LN-10), which is driven by the sum of two sinusoidal FM signals generated from an arbitrary waveform generator (AWG - Keysight M8195A). The two FM signals are centered at 6 GHz with a frequency deviation (Δf) of 2 GHz each. The modulation frequencies of the two FM signals are varied between 71 kHz and 80 kHz, which corresponds to a measurement range and spatial resolution of about 1.3 km and 6 m respectively according to Eqs. (1) and (2). The output of the phase modulator is filtered using a bandpass filter (BPF_1 - Finisar WaveShaper 1000S) to extract the desired frequency modulated optical signals (shown in inset of Fig. 2) which are subsequently split into pump and probe waves. The pump lightwave after amplification is launched from one end of the FUT consisting of a 1 km long fiber (Fiber 1) followed by a 100 m long fiber (Fiber 2). The probe lightwave on the other arm is passed through 14 km long delay fiber so that the correlation peak generated within the FUT corresponds to non-zeroth order interaction. The delayed probe is

Optics EXPRESS

amplified, frequency shifted by the Brillouin frequency (f_B) using an electro-optic modulator (EOM) in carrier suppressed configuration and is launched from the other end of the FUT.

The frequency modulated pump and probe interact in the FUT and generate multiple correlation peaks at locations determined by the carefully chosen f_m frequencies. The amplified probe is filtered using a fiber Bragg grating to extract the Brillouin Stokes component and is detected using a 45 MHz photo receiver. Lock-in detection at $2f_m$ frequency is performed using an electrical spectrum analyzer (ESA - R&S FSV30) in zero-span mode.

4. Results

4.1. Spatial mapping of multiple correlation peaks

As mentioned in the Introduction, one of the key objectives of this work is to generate multiple and independent correlation peaks in the FUT simultaneously. In order to verify the generation and independent control of multiple correlation peaks, the Brillouin gain at a particular pump-probe frequency offset is spatially mapped which gives the location and profile of the generated correlations [19]. In order to enable spatial mapping, we modulate the pump with a narrow pulse train (50 ns pulsewidth, 11 μs period) using an EOM [19] and observe the amplified probe on an oscilloscope. It should be noted that the pulsing of pump is implemented only to observe the spatial profile of the correlations and is not implemented in the actual sensing experiments which are discussed in the subsequent sections. The phase modulator is driven with two sinusoidal FM signals with modulation frequencies (f_m) of 84 kHz and 94 kHz respectively and Δf of 500 MHz each, which corresponds to a measurement range and spatial resolution of 1.1 km and 21 m respectively according to Eq. (1) and (2). The amplified probe trace observed on an oscilloscope for 10.800 GHz frequency offset between pump and probe with only Fiber 1 (~1 km) as FUT is shown in Fig. 3 [17]. Note that the time axis in the plot is translated to corresponding distances using the time of flight of pump.

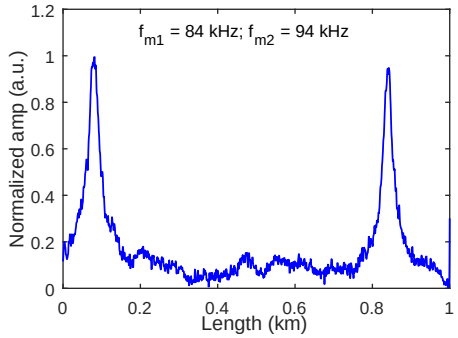

Fig. 3. Amplified probe trace obtained by pulsing the pump showing two correlation peaks when phase modulator is driven with two FM signals [17].

The trace contains two distinct peaks indicating that two correlation peaks are generated due to the two FM signals at locations determined by the respective modulation frequencies (f_{m1} and f_{m2}). The width of the correlation features are 40 m and 34 m respectively which have been verified independently through simulations. In order to demonstrate the independent tunability of the two correlation peaks, the modulation frequency (f_{m2}) of one of the FM signals is varied from 84 kHz to 94 kHz while that of the other is unchanged. The amplified probe traces obtained are shown in Fig. 4(a) [17].

The location of correlation peak corresponding to the varying modulation frequency f_{m2} alone has changed while the one due to the fixed modulation frequency f_{m1} remain unchanged. This has been also checked by keeping the modulation frequency f_{m2} fixed and varying the other

Optics EXPRESS

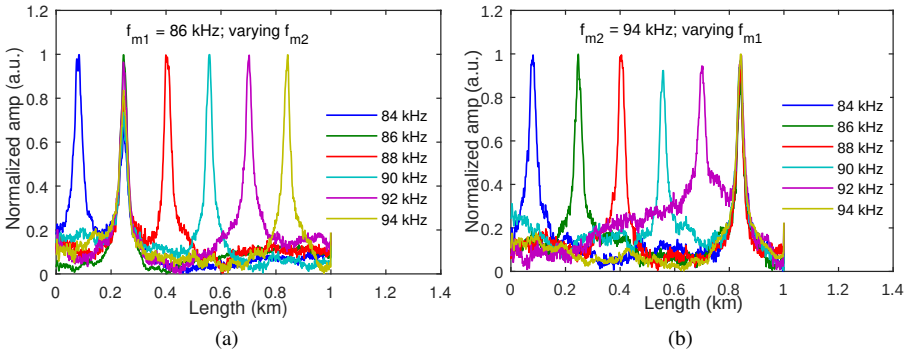

Fig. 4. Amplified probe traces with (a) fixed f_{m1} and varying f_{m2} (b) fixed f_{m2} and varying f_{m1} showing the independent tunability of the two correlation peaks [17].

modulation frequency f_{m1} as shown in Fig. 4(b). As expected, the width of each correlation feature is observed to change from 40 m to 34 m with change in f_m from 84 kHz to 94 kHz. Both the results of Fig. 4 clearly demonstrate that multiple correlation peaks generated through external modulation-based BOCDA can be tuned independently.

4.2. *Sensing of static strain from multiple correlation peaks*

In order to detect static strain variations using external modulation-based BOCDA, Fiber 2 (~100 m) is added to the FUT consisting of Fiber 1 (~1 km). FM signals with modulation frequencies between 70 kHz and 80 kHz are used to ensure that only one correlation peak is generated within the FUT due to each of the FM signals. Varying the modulation frequency from 71 kHz to 79 kHz sweeps the correlation peak across the Fiber 1 and with a modulation frequency closer to 80 kHz, the other correlation peak is localized within Fiber 2. In order to obtain the BGS and estimate the BFS along the FUT, the phase modulator is initially driven by one FM signal with Δf of 2 GHz. The spectrum of the amplified probe after photo detection with a modulation frequency of 75 kHz is shown in Fig. 5.

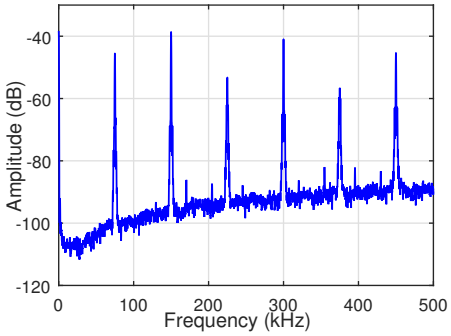

Fig. 5. Spectrum recorded at the output of the photo detector when phase modulator is driven with one FM signal with f_m of 75 kHz.

The spectrum consists of distinct peaks at a frequency of f_m and its harmonics. The frequency offset between pump and probe is varied from 10.701 GHz to 10.900 GHz in steps of 1 MHz and the corresponding BGS is captured using the ESA in zero-span mode locked to $2f_m$ frequency. The BGS is acquired for different f_m values which sweeps the correlation peak along the 1.1 km

Optics EXPRESS

long FUT. The BGS traces and the corresponding BFS obtained from peak detection at different locations are shown in Fig. 6.

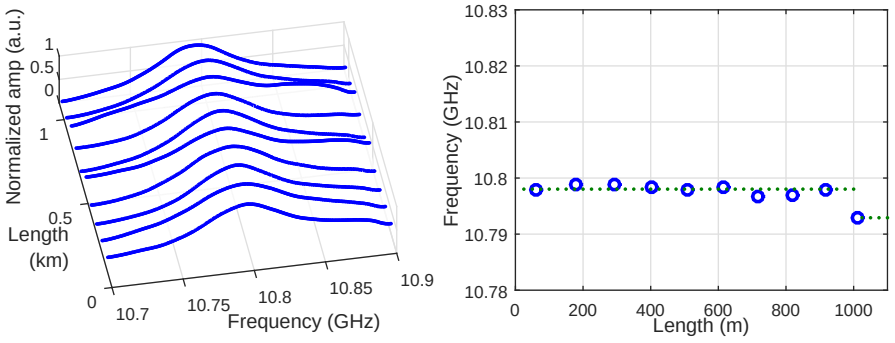

Fig. 6. (a) BGS along 1.1 km long FUT obtained by varying f_m from 71 kHz to 80 kHz and (b) the corresponding BFS as a function of the sensing fiber length.

The BFS of Fiber 1 is nearly 10.798 GHz while that of Fiber 2 is slightly lower (~10.793 GHz). The BFS of these fibers are measured independently through Brillouin optical time domain analysis measurements which are in good agreement with these values. We then proceed to drive the phase modulator with two sinusoidal FM signals centered at 6 GHz with f_m frequencies of 75 kHz and 80.5 kHz such that correlation peaks are generated in the 1 km fiber and 100 m fiber respectively. Fiber 2 is wound across two posts mounted on translational stages and static strain is applied by moving one of the stages. The BGS traces obtained by locking ESA to the corresponding $2f_m$ frequencies in zero-span mode are shown in Fig. 7.

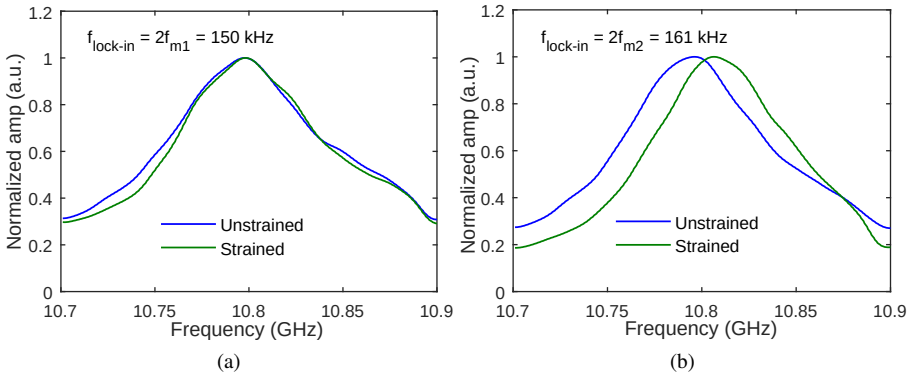

Fig. 7. BGS traces corresponding to the correlation peaks at (a) 510 m and (b) 1057 m generated using f_{m1} = 75 kHz and f_{m2} = 80.5 kHz respectively when strain is applied on Fiber 2.

Due to strain in Fiber 2, the BGS of the correlation peak location within Fiber 1 has not shifted while that in Fiber 2 has shifted by 10.1±0.8 MHz which corresponds to a strain perturbation of 202±16 $\mu\epsilon$. Such a strain perturbation on Fiber 2 is verified independently using a fiber Bragg grating embedded in the sensing fiber. These experiments validate our proposed technique of external modulation-based BOCDA to measure strain at independent locations in the fiber; the BGS obtained from each correlation peak is dependent only on the strain applied at that

Optics EXPRESS

location. Due to the presence of multiple frequency modulated signals in the system, there could be an increase in beat noise when compared to a system with single correlation peak. However, the lock-in detection process still allows the precise extraction of BGS from multiple locations as shown in Figs. 7(a) and 7(b). Although in the above experiments, sensing is done at two specific locations decided by the chosen f_m frequencies, the same can be implemented at any two locations within the FUT by choosing appropriate modulation frequencies, f_{m1} and f_{m2}. For instance, in order to sense the strain variations at 290 m and 615 m within the FUT, the phase modulator has to be driven with two FM signals with f_m frequencies of 73 kHz and 76 kHz.

4.3. Sensing of dynamic strain from multiple correlation peaks

In order to demonstrate the capability of external modulation-based BOCDA in detecting dynamic strain variations at multiple locations, dynamic strain is emulated in Fiber 2 by switching the optical path [20] between two fibers whose Brillouin frequencies differ by 40 MHz approximately. The FUT is shown in Fig. 8 where an optical switch (oeMarket - OSW-W1×2; T_{switch}> 5 ms) is used to emulate dynamic strain in the 100 m long fiber.

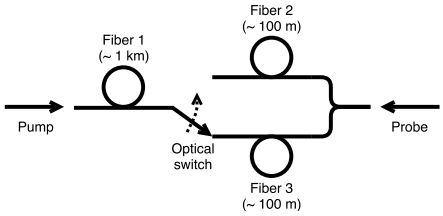

Fig. 8. FUT to emulate dynamic strain over 100 m long fiber using an optical switch.

Similar to the static strain measurements, two sinusoidal FM signals are used with f_m frequencies of 75 kHz and 80.5 kHz and Δf of 2 GHz each such that two correlation peaks are generated - one each in the 1 km fiber and the 100 m fiber. The optical path is switched between the two 100 m fibers, every 500 ms (switching frequency = 1 Hz). The frequency offset between pump and probe is varied from 10.701 GHz to 10.900 GHz in steps of 3 MHz; this process takes about 210 ms for each BGS measurement, limited only by the sweeping time of the probe frequency in our setup. Fig. 9 shows the BGS traces and the corresponding BFS as a function of time obtained through lock-in detection at the corresponding $2f_m$ frequencies.

The BGS of the correlation peak location within Fiber 1 is observed to remain unchanged as seen from Fig. 9(a) and the corresponding BFS is almost constant as a function of time (Fig. 9(c)). On the other hand, the BGS of the correlation peak generated within Fiber 2 is found to be switching periodically as seen from Fig. 9(b) and the corresponding BFS is in good agreement with the square wave fitting with a switching frequency of 1 Hz (Fig. 9(d)). The standard deviation in the estimated BFS is nearly 1.2 MHz. This demonstrates the multi-point dynamic strain sensing capability of the external modulation-based BOCDA technique.

We then proceed to switch the optical path, every 150 ms (switching frequency = 3.3 Hz). As explained earlier, a scan over 200 MHz with a step size of 3 MHz in the probe frequency requires a minimum of 210 ms. In order to resolve a dynamic strain at 3.3 Hz, we increase this step size to 10 MHz resulting in a BGS measurement time of 65 ms. The BGS traces and the corresponding BFS are shown in Fig. 10. The BGS traces obtained are as predicted and the BFS of the correlation peak location within Fiber 2 is in good agreement with the expected square wave fitting. The standard deviation in the estimated BFS is nearly 2 MHz.

In the above experiments, the maximum rate of BFS variations that can be detected is limited by the finite sweeping time of the frequency offset between the pump and the probe. However, in situations where measurement of the absolute amplitude of strain is not very critical, perturbations

Optics EXPRESS

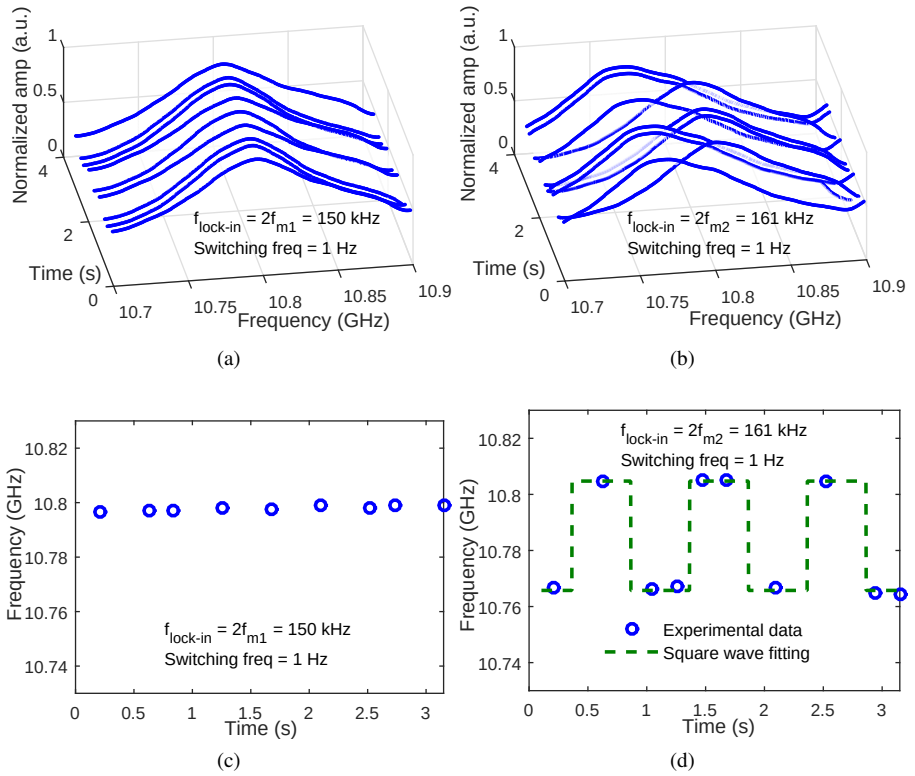

Fig. 9. BGS traces of the correlation peak location within (a) Fiber 1 (f_{m1} = 75 kHz) and (b) Fiber 2 (f_{m2} = 80.5 kHz) when Fiber 2 is subjected to dynamic strain with a switching frequency of 1 Hz. The corresponding BFS as a function of time are shown in (c) and (d). Step size of probe frequency scanning is 3 MHz.

at higher rates can be detected by measuring the intensity variations of the amplified probe at a specific pump-probe frequency offset. In order to demonstrate this, the optical path is switched between the two 100 m fibers every 10 ms (switching frequency = 50 Hz) and the frequency offset between the pump and the probe is fixed at 10.750 GHz. The amplified probe at a lock-in frequency of 161 kHz is monitored as a function of time and is shown in Fig. 11(a).

The amplitude variations shown in Fig. 11(a) resemble a square wave with a frequency of 50 Hz which closely matches the frequency of dynamic strain variations. The extinction of the trace is nearly 3 dB, consistent with the change in Brillouin gain corresponding to the BGS shift as seen from the BGS traces in Fig. 11(b). The rate of dynamic strain variations detected is limited by the switching speed of the optical switch used. Thus the external modulation-based BOCDA technique is suitable to detect dynamic strain variations at multiple locations.

In all the above experiments, an electrical spectrum analyzer in the zero-span mode is used as a single channel lock-in amplifier (LIA) where the two correlation peaks are monitored sequentially by only changing the lock-in frequency. In order to achieve *simultaneous* monitoring of dynamic strain variations at two different locations, we need another independent channel locking into the second modulation frequency as well. The experimental details for such a demonstration with sub-meter spatial resolution are explained below. The length of the FUT chosen for this experiment is 100 m, consisting of two standard singlemode fiber spans of 90 m (Fiber 1) and 10 m (Fiber 2 or Fiber 3) respectively. The length of the delay fiber used is 1.3 km. The phase

Optics EXPRESS

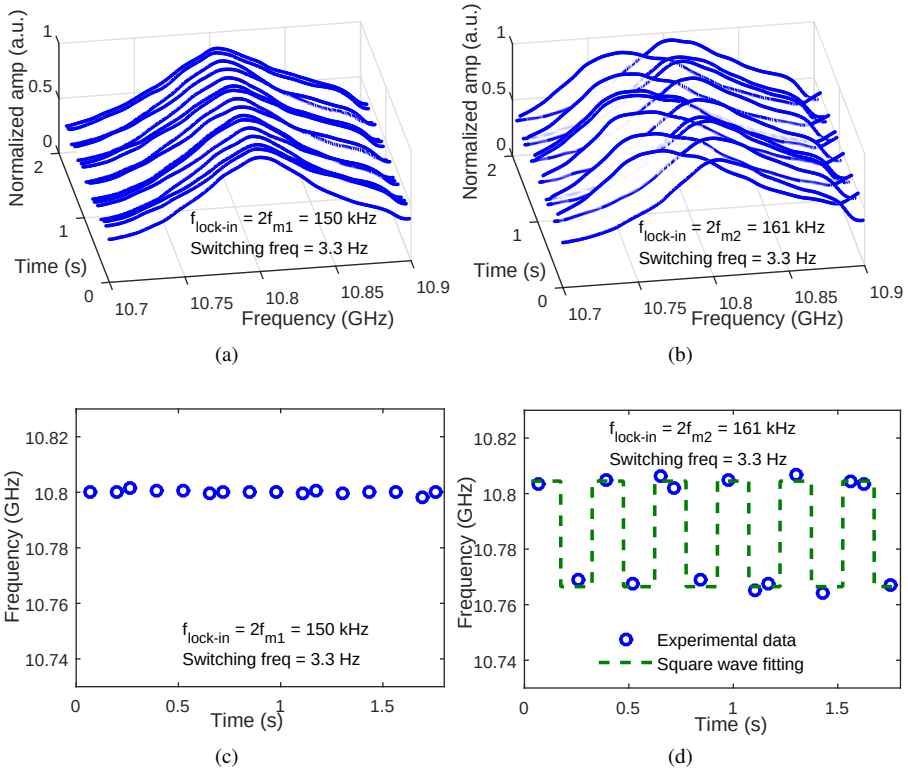

Fig. 10. BGS traces of the correlation peak location within (a) Fiber 1 (f_{m1} = 75 kHz) and (b) Fiber 2 (f_{m2} = 80.5 kHz) when Fiber 2 is subjected to dynamic strain with a switching frequency of 3.3 Hz. The corresponding BFS as a function of time are shown in (c) and (d). Step size of probe frequency scanning is 10 MHz.

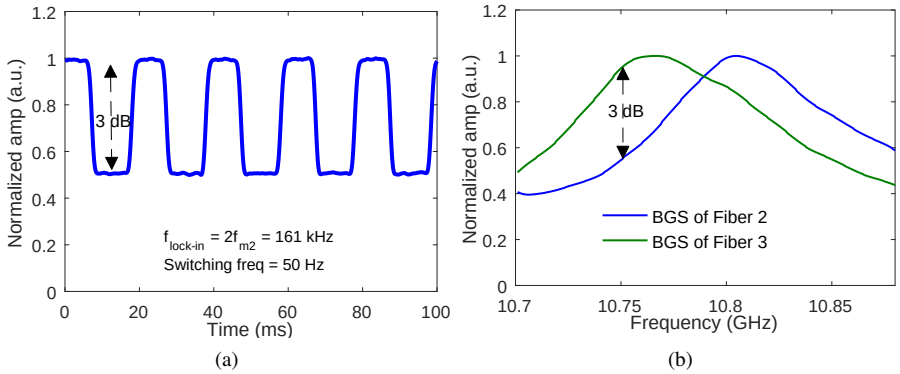

Fig. 11. (a) Amplified probe at a lock-in frequency of 161 kHz at a fixed pump-probe frequency offset of 10.750 GHz, when Fiber 2 is subjected to dynamic strain with a switching frequency of 50 Hz. BGS of the two fibers are shown in (b) for reference.

Optics EXPRESS

modulator is driven with two FM signals with modulation frequencies of 730 kHz (f_{m1}) and 845 kHz (f_{m2}), and frequency deviation of 2 GHz each, resulting in two correlation peaks - one each in the 90 m fiber and the 10 m fiber with a width of ~60 cm. This has been verified independently through the spatial mapping of correlation peaks technique discussed in Section 4.1. The optical path is switched between the two 10 m fibers, every 250 ms (switching frequency = 2 Hz) to simulate the dynamic variations in the Brillouin frequency. The frequency offset between pump and probe is varied from 10.701 GHz to 10.900 GHz in steps of 1 MHz. Since we did not have access to a multi-channel LIA, we followed the following approach to monitor the BGS at two locations simultaneously. The output of the photo detector shown in Fig. 2 is split into two parts - one connected to the electrical spectrum analyzer in zero-span mode and the other connected to an LIA (SR844) followed by an oscilloscope. The lock-in frequency of LIA is set to 1460 kHz ($2f_{m1}$) and the center frequency of ESA in zero-span mode is set to 1690 kHz ($2f_{m2}$) such that the BGS of the two locations are monitored simultaneously.

Figs. 12(a) and 12(b) show the BGS of the two different fiber sections obtained simultaneously through lock-in detection at the corresponding $2f_m$ frequencies, which are consistent with expectations. The corresponding BFS as a function of time for the two fiber sections are shown in Figs. 12(c) and 12(d) respectively. We observe that the BFS in Fiber 1 does not change with time,

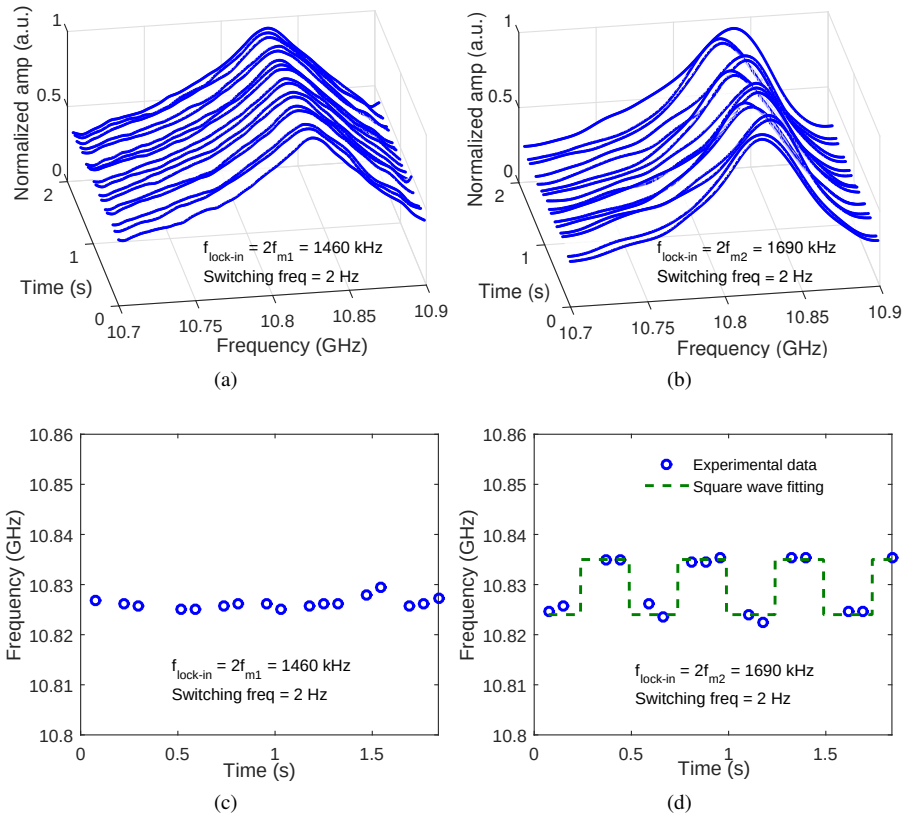

Fig. 12. BGS traces of the correlation peak location within (a) Fiber 1 (f_{m1} = 730 kHz) and (b) Fiber 2 (f_{m2} = 845 kHz) obtained simultaneously when Fiber 2 is subjected to dynamic strain with a switching frequency of 2 Hz. The corresponding BFS as a function of time are shown in (c) and (d). Step size of probe frequency scanning is 1 MHz.

whereas the BFS in Fiber 2 changes according to the applied switching frequency. The observed

Optics EXPRESS

BFS in Fiber 2 is in good agreement with the expected square wave fit, with a standard deviation of ~1.2 MHz. This demonstrates the capability of external modulation-based BOCDA in sensing multiple dynamic strain variations simultaneously with sub-meter spatial resolution. It should be noted that the demonstration of finer spatial resolution is limited only by the bandwidth of the available modulator driver and phase modulator, and does not pose any fundamental limitation.

5. Discussion

From the above demonstrations, it is evident that the external modulation-based BOCDA is a promising technique to detect dynamic strain variations at multiple locations simultaneously. For the proof-of-principle experiments demonstrated in this paper, the measurement range is 100 m and the spatial resolution is 60 cm as decided by the choice of f_m and Δf. The technique can further be extended to smaller FUT and sensing with better spatial resolution by choosing appropriate FM parameters. For instance, a measurement range of 10 m with a spatial resolution of 2 cm can be achieved with an f_m in the range of 10 MHz and Δf of 5 GHz. Another key aspect of this technique is that it is scalable and can be used to monitor the strain in multiple locations by generating multiple correlation peaks with appropriate sets of f_m and Δf. In the dynamic strain sensing experiments discussed above, the strain at one location is dynamic whereas at the other is static. It should be noted that the proposed technique can be implemented even when multiple locations are subjected to dynamic strain perturbations. In a typical BOCDA implementation, the highest measured frequency of dynamic strain is limited by the sampling rate of the receiver. In case of conventional BOCDA, simultaneous measurement of dynamic strain from two different sensing points would require a proportionately higher sampling rate. In contrast, the external modulation-based BOCDA provides a pathway to scale the number of sensing points while maintaining the original sampling rate, thereby preserving the maximum detectable frequency of dynamic strain at each sensing point.

While the above discussion points to several exciting pathways for further performance improvement of the external modulation-based BOCDA technique, one should be also aware of a few limitations on the scaling of the number of sensing points. As seen from the above experiments, monitoring of multiple locations simultaneously requires lock-in detection at a specific frequency for each of the locations to be monitored. This requires multiple lock-in amplifiers which poses a significant challenge for practical implementation. One way of potentially overcoming this limitation is through the use of a multi-channel lock-in amplifier with an appropriately different lock-in frequency in each channel [21].

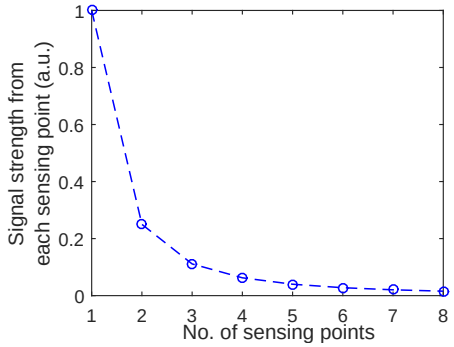

Fig. 13. Strength of signal from each sensing point for varying number of sensing points (N) when external modulation-based BOCDA is implemented. The signal strength is normalized to that when one sensing point is monitored ($N = 1$).

Another serious limitation in scaling the number of sensing points is that the available RF

Optics EXPRESS

and optical power levels are shared among multiple FM signals used to simultaneously generate multiple correlation peaks. This leads to a significant reduction in the strength of the signal from each sensing point as we attempt to scale the number of sensing points as shown in Fig. 13, which in turn results in a degradation of the signal-to-noise ratio (SNR) from each correlation peak. Typically, this is overcome by increasing the averaging in order to maintain the same accuracy in BFS estimation. However, the averaging process takes time and hence compromises the advantage of simultaneous multi-point sensing provided by the external modulation-based BOCDA technique. Post processing techniques based on linear approximation approach [22] and gradient descent method [23] are being studied to estimate the BFS accurately even at lower SNR, thereby avoiding the need for increased averaging.

6. Conclusion

In this paper, we demonstrate a novel technique for multi-point sensing of dynamic strain variations using external modulation-based BOCDA which provides a clear pathway for simultaneous monitoring of multiple sensing locations in an independent manner. Multiple frequency modulations are generated with appropriate f_m and Δf values in the electrical domain, which are further transferred to the pump and the probe using external phase modulation. The BGS from multiple correlation peak locations are shown to be independent in the detection of strain variations through controlled experiments. Two correlation peaks each 6 m wide, whose locations can be tuned independently are generated within the 1.1 km long FUT. The static strain variations at the two correlation peak locations are detected independently through lock-in detection at a frequency corresponding to twice the modulation frequency. We demonstrate the detection of dynamic BFS variations at 3.3 Hz, only limited by the 65 ms sweep time of the probe frequency in our setup. By fixing the frequency offset between the pump and the probe, we demonstrate our capability to detect BFS variations at a rate of 50 Hz (limited by the speed of the optical switch used). We also demonstrate the detection of dynamic strain variations at 2 Hz at two locations simultaneously with 60 cm spatial resolution over 100 m long FUT. Based on the above results, we conclusively prove that the external modulation-based BOCDA technique is a viable solution for simultaneous monitoring of dynamic strain variations at multiple independent locations in a fiber.

Appendix A

Generation of multiple correlation peaks

Consider the generation of two correlation peaks within the sensing fiber at two locations determined by the two modulation frequencies f_{m1} and f_{m2}. The desired electric field of the pump at the input of the sensing fiber is given by

$$E_{in}(t) = E_1 \exp\left[j\left\{(\omega_c + \omega_1)t + \frac{\Delta f_1}{f_{m1}} \sin\left(2\pi f_{m1} t\right)\right\}\right] + E_2 \exp\left[j\left\{(\omega_c + \omega_2)t + \frac{\Delta f_2}{f_{m2}} \sin\left(2\pi f_{m2} t\right)\right\}\right], \quad (3)$$

where E_1 and E_2 are the amplitudes, ω_c is the angular frequency of the optical carrier, ω_1 and ω_2 are the angular frequency difference between the optical carrier and center of two FM signals respectively, f_{m1} and f_{m2} are the modulation frequencies; and Δf_1 and Δf_2 are the frequency deviations of the two FM signals. The probe can be obtained by frequency shifting the pump by Brillouin frequency with an EOM in carrier suppressed configuration.

Consider the case of generating the multiple FM signals in optical domain using the direct modulation of a light source. When the light source is modulated with a current consisting of

Optics EXPRESS

sum of two sinusoids as shown below,

$$I(t) = I_0 + I_1 \cos\left(2\pi f_{m1} t\right) + I_2 \cos\left(2\pi f_{m2} t\right), \tag{4}$$

the corresponding electric field at the output of the laser is given by

$$E_{laser}(t) = E_0 \exp\left[j\left\{\omega_c t + \frac{\Delta f_1}{f_{m1}} \sin\left(2\pi f_{m1} t\right) + \frac{\Delta f_2}{f_{m2}} \sin\left(2\pi f_{m2} t\right)\right\}\right], \tag{5}$$

which is not the same as in Eq. (3). The electric field consists of only one carrier and hence cannot generate two FM signals simultaneously. Hence the direct modulation of a light source is not a viable solution in generating multiple independently-addressable correlation peaks.

Now consider the case of generating the same using an external phase modulator. When the voltage signal driving the phase modulator consists of sum of two FM signals as shown below,

$$V(t) = V_0\left[\sin\left\{\omega_1 t + \frac{\Delta f_1}{f_{m1}} \sin\left(2\pi f_{m1} t\right)\right\} + \sin\left\{\omega_2 t + \frac{\Delta f_2}{f_{m2}} \sin\left(2\pi f_{m2} t\right)\right\}\right] \tag{6}$$

the electric field at the output of the phase modulator is given by

$$E_{mod}(t) = E_0 \exp\left(j\omega_c t\right) \exp\left(j\frac{\pi V(t)}{V_\pi}\right) \tag{7}$$

where V_π is the half-wave voltage of the phase modulator. On expanding the second term using Taylor series, the electrical field is as below.

$$E_{mod}(t) = E_0 \exp\left(j\omega_c t\right)\left(1 + j\frac{\pi V(t)}{V_\pi} + \ldots\right) \tag{8}$$

On substituting $V(t)$ with that in Eq. (6), expanding $\sin(\theta)$ and rearranging the terms, the electric field can be written as follows.

$$\begin{aligned} E_{mod}(t) = E_0 \exp(j\omega_c t) + E_1 \Bigg[& \exp\left\{j\left((\omega_c + \omega_1)t + \frac{\Delta f_1}{f_{m1}} \sin\left(2\pi f_{m1} t\right)\right)\right\} \\ & + \exp\left\{j\left((\omega_c + \omega_2)t + \frac{\Delta f_2}{f_{m2}} \sin\left(2\pi f_{m2} t\right)\right)\right\}\Bigg] \\ & - E_1 \Bigg[\exp\left\{j\left((\omega_c - \omega_1)t - \frac{\Delta f_1}{f_{m1}} \sin\left(2\pi f_{m1} t\right)\right)\right\} \\ & + \exp\left\{j\left((\omega_c - \omega_2)t - \frac{\Delta f_2}{f_{m2}} \sin\left(2\pi f_{m2} t\right)\right)\right\}\Bigg] + \ldots \end{aligned} \tag{9}$$

If the higher order terms are filtered, then the electric field of the output of phase modulator consists of an optical carrier and multiple FM signals each at a center frequency of $\omega_c \pm \omega_1$ and $\omega_c \pm \omega_2$ with f_m and Δf decided by those corresponding to the voltage signals used to drive the phase modulator. Filtering higher frequencies can be achieved in the optical domain. Hence by using an external phase modulator, multiple FM signals in the electrical domain can be embedded in the optical domain and hence can be used to generate multiple independently-addressable correlation peaks.

Appendix B

Simulation results

One of the key challenges in monitoring multiple locations simultaneously is the extraction of the strain information from multiple sensing locations without significant cross-talk. Simulations

Optics EXPRESS

are performed to verify the dependence of BGS from each correlation peak with that of the other correlation peaks in the FUT. We extend the methodology followed in [19] to simulate the SBS interaction over 1 km long fiber and estimate the amplified probe when the two lightwaves - pump and probe are modulated with multiple sinusoidal FM signals. Under undepleted pump approximation, SBS interaction between pump and probe is modeled using the steady-state propagation equations [24]. The amplified probe power is computed using the pump power and SBS gain which depends on the local BFS and the instantaneous frequency offset between pump and probe [25].

The time step size considered is 5 ns which corresponds to space step size of 1 m. The BFS of the fiber is considered as 10.800 GHz. The pump and the probe are considered to be modulated with a sinusoidal FM signal centered at 6 GHz with an f_m frequency of 74 kHz and Δf of 2 GHz. The probe is delayed by 70 μs relative to the pump. This generates a correlation peak at 450 m within the FUT as per Eq. (1). The spectrum of simulated amplified probe contains distinct components at f_m frequency i.e., 74 kHz and its harmonic frequencies. In order to find the optimum frequency for lock-in detection, the frequency offset between pump and probe is varied from 10.70 GHz and 10.90 GHz and the amplified probe is simulated at all the frequency offsets and at different lock-in frequencies which are shown in Fig. 14.

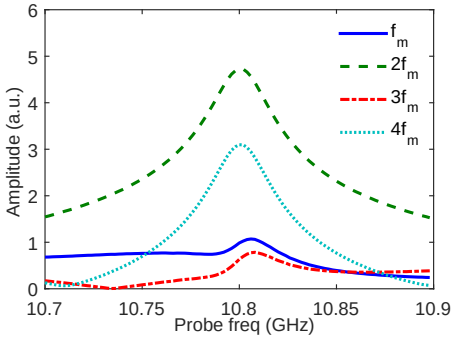

Fig. 14. Amplified probe traces at different lock-in frequencies for varying frequency offset between pump and probe; BFS is assumed to be 10.800 GHz.

The trace obtained with lock-in detection at $2f_m$ and $4f_m$ frequencies resemble the BGS with a BFS of 10.800 GHz and among the two, the one corresponding to $2f_m$ frequency exhibits larger strength, leading to potentially higher signal-to-noise ratio and hence better accuracy in the estimation of BFS. This is expected because the pump and the probe are frequency modulated at f_m and are counter propagated in the FUT. The BGS which is formed due to the correlation between the two lightwaves, is expected to have components at $2f_m$ frequency and its harmonics.

In order to verify the dependence of BGS from a correlation peak location on that of the other correlation peak locations, the pump and probe are considered to be modulated with two sinusoidal FM signals centered at 6 GHz with f_m frequencies 74 kHz and 78 kHz and Δf of 2 GHz each. The probe is delayed by 70 μs relative to the pump. This generates two correlation peaks at 450 m and 800 m as per Eq. (1). The spatial resolution, given by the width of correlation (Eq. (2)), is nearly 6 m each. The frequency offset between pump and probe is varied from 10.700 GHz to 10.900 GHz. A strain perturbation equivalent to an increase in BFS of 10 MHz is simulated at the correlation peak location which corresponds to an f_m frequency of 74 kHz. The BGS traces are obtained by simulating lock-in detection [26] at the corresponding $2f_m$ frequencies.

The BGS at the two correlation peak locations obtained through simulations in the presence and absence of strain are shown in Fig. 15.

Optics EXPRESS

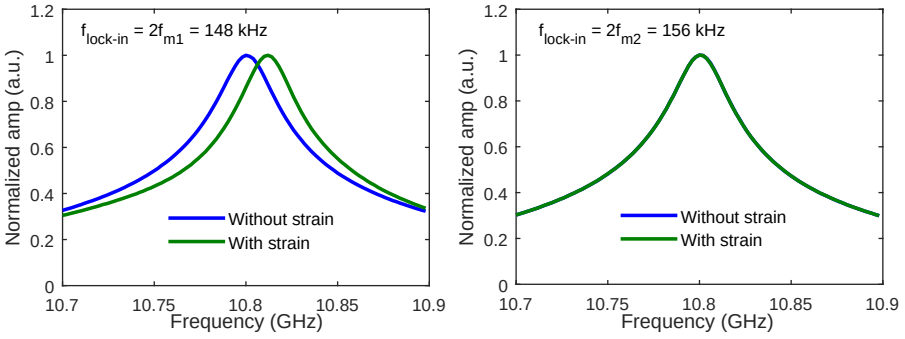

(a) (b)

Fig. 15. Simulated BGS traces at correlation peak locations corresponding to (a) f_{m1} = 74 kHz and (b) f_{m2} = 78 kHz. Strain is simulated at the location corresponding to the correlation peak at f_{m1} = 74 kHz. BGS traces are obtained through lock-in detection corresponding to $2f_m$ frequencies.

In the absence of strain, the BFS at the two locations is 10.800 GHz. In the presence of strain, the peak of the BGS at the correlation peak location corresponding to a modulation frequency of 74 kHz is shifted to 10.81 GHz while the other peak corresponding to a modulation frequency of 78 kHz has not shifted. This conveys that the BGS of each correlation peak location is independent on the BGS of the other correlation peak locations. These results are validated through experiments as described in Sections 3 and 4.

Funding

Department of Electronics and Information Technology (DeitY, Govt. of India); Ministry of Human Resource Development (MHRD, Govt. of India); Department of Science and Technology (DST, Govt. of India); Office of the Principal Scientific Advisor - Govt. of India.

Acknowledgments

Authors would like to thank Dr K V Reddy, PriTel Inc., USA for providing the optical amplifier and Prof Wei Jin, Department of Electrical Engineering, The Hong Kong Polytechnic University, Hong Kong for providing the lock-in amplifier.

References

1. T. Horiguchi, T. Kurashima, and M. Tateda, "A technique to measure distributed strain in optical fibers," IEEE Photonics Technol. Lett. **2**, 352–354 (1990).
2. T. Kurashima, T. Horiguchi, and M. Tateda, "Distributed-temperature sensing using stimulated Brillouin scattering in optical silica fibers," Opt. Lett. **15**, 1038–1040 (1990).
3. M. Nikles, L. Thévenaz, and P. A. Robert, "Simple distributed fiber sensor based on Brillouin gain spectrum analysis," Opt. Lett. **21**, 758–760 (1996).
4. M. N. Alahbabi, Y. T. Cho, and T. P. Newson, "150-km-range distributed temperature sensor based on coherent detection of spontaneous Brillouin backscatter and in-line Raman amplification," J. Opt. Soc. Am. B **22**, 1321–1324 (2005).
5. X. Bao and L. Chen, "Recent progress in Brillouin scattering based fiber sensors," Sensors (Basel) **11**, 4152–4187 (2011).
6. K. Hotate and T. Hasegawa, "Measurement of Brillouin gain spectrum distribution along an optical fiber using a correlation-based technique–proposal, experiment and simulation," IEICE Trans. Electron. **E83-C**, 405–412 (2000).
7. A. Zadok, Y. Antman, N. Primerov, A. Denisov, J. Sancho, and L. Thevenaz, "Random-access distributed fiber sensing," Laser & Photonics Rev. **6**, L1–L5 (2012).
8. K. Y. Song and K. Hotate, "Distributed fiber strain sensor with 1-kHz sampling rate based on Brillouin optical correlation domain analysis," IEEE Photonics Technol. Lett. **19**, 1928–1930 (2007).

Optics EXPRESS

9. H. Guo, G. Xiao, N. Mrad, and J. Yao, "Fiber optic sensors for structural health monitoring of air platforms," Sensors **11**, 3687–3705 (2011).
10. K. Hotate and M. Tanaka, "Distributed fiber Brillouin strain sensing with 1-cm spatial resolution by correlation-based continuous-wave technique," IEEE Photonics Technol. Lett. **14**, 179–181 (2002).
11. Y. Antman, N. Primerov, J. Sancho, L. Thévenaz, and A. Zadok, "Localized and stationary dynamic gratings via stimulated Brillouin scattering with phase modulated pumps," Opt. Express **20**, 7807–7821 (2012).
12. K. Y. Song, Z. He, and K. Hotate, "Optimization of Brillouin optical correlation domain analysis system based on intensity modulation scheme," Opt. Express **14**, 4256–4263 (2006).
13. M. Tanaka and K. Hotate, "Application of correlation-based continuous-wave technique for fiber Brillouin sensing to measurement of strain distribution on a small size material," IEEE Photonics Technol. Lett. **14**, 675–677 (2002).
14. K. Hotate and S. S. Ong, "Distributed dynamic strain measurement using a correlation-based Brillouin sensing system," IEEE Photonics Technol. Lett. **15**, 272–274 (2003).
15. G. Ryu, G.-T. Kim, K. Y. Song, S. B. Lee, and K. Lee, "Brillouin optical correlation domain analysis enhanced by time-domain data processing for concurrent interrogation of multiple sensing points," J. Lightwave Technol. **35**, 5311–5316 (2017).
16. D. Elooz, Y. Antman, N. Levanon, and A. Zadok, "High-resolution long-reach distributed Brillouin sensing based on combined time-domain and correlation-domain analysis," Opt. Express **22**, 6453–6463 (2014).
17. B. Somepalli, D. Venkitesh, and B. Srinivasan, "Simultaneous multi-point sensing through external phase modulation based Brillouin optical correlation domain analysis," in *Asia Communications and Photonics Conference,* (Optical Society of America, 2017), pp. M2A–3.
18. K. Hotate, "Fiber distributed Brillouin sensing with optical correlation domain techniques," Opt. Fiber Technol. **19**, 700–719 (2013).
19. B. Somepalli, D. Venkitesh, and B. Srinivasan, "Spatial mapping of correlation profile in Brillouin optical correlation domain analysis," Meas. Sci. Technol. **28**, 045202 (2017).
20. C. Kito, H. Takahashi, K. Toge, and T. Manabe, "Dynamic strain measurement of 10-km fiber with frequency-swept pulsed BOTDA," J. Lightwave Technol. **35**, 1738–1743 (2017).
21. M. O. Sonnaillon and F. J. Bonetto, "A low-cost, high-performance, digital signal processor-based lock-in amplifier capable of measuring multiple frequency sweeps simultaneously," Rev. Sci. Instruments **76**, 024703 (2005).
22. B. Somepalli, D. Venkitesh, U. Khankhoje, and B. Srinivasan, "Deconvolution algorithm for accurate estimation of Brillouin frequency in Brillouin optical correlation domain analysis," in *Optical Fiber Sensors,* (Optical Society of America, 2018), p. ThE20.
23. J. Nocedal and S. J. Wright, *Numerical Optimization* (Springer, 2006).
24. G. P. Agrawal, *Nonlinear Fiber Optics* (Academic, 2007).
25. R. W. Boyd, *Nonlinear Optics* (Academic, 2003).
26. J. H. Jeong, K. Lee, K. Y. Song, J.-M. Jeong, and S. B. Lee, "Variable-frequency lock-in detection for the suppression of beat noise in Brillouin optical correlation domain analysis," Opt. Express **19**, 18721–18728 (2011).